Al Azhar Bulletin of Science Vol.(25) No.1, June, 29 - 46, 2014,.

CONTRIBUTION TO THE MIERALOGY AND RADIOACTIVITY OF STREAM SEDIMENTS OF WADI RAS BAROUD AREA, NORTH EASTERN DESERT, EGYPT

El Azab, A., Omran, A. and Hassan, A. H

Nuclear Materials Authority. P.O. Box 530, El Maadi, Cairo, Egypt.

ABSTRACT

Wadi Ras Baroud area is located in the North Eastern Desert of Egypt, covering an area of about 170km2. It is covered by basement rocks and dissected by several wadies. The rock assemblages cropping out at Wadi Ras Baroud area comprise, quartz diorites, granodiorites, syenogranites, dykes and Quaternary sediments filling the streams of the studied area.

The grain size analysis and their distribution is a fundamental descriptive measure for clastic sediments. The results of the statistical parameters are a graphic mean (Mz) ranging from 0.4φ to2φ, inclusive graphic standard deviation (σI) ranging from 1.2 to 1.9, inclusive graphic skewness (SkI) ranging from -0.3 to 0.22, and inclusive graphic kurtosis (Kg) ranging from 0.7 to 1.1. These parameters clear that they are coarse to medium sand, poorly sorted, near to coarse skewed samples, and platykurtic and mesokurtic, so these sediments are represented by the turbidity currents environments.

The identified minerals in the heavy fractures are represented by magnetite, ilmenite, hematite, garnet, rutile, titanite, zircon, thorite, ferogusnite, and columbite. The radiometric study of the stream sediments of Wadi Ras Baroud indicates that the average concentrations of U and Th are 10.38ppm and 25.5ppm respectively.

INTRODUCTION

Ras Baroud area is located in the North Eastern Desert of Egypt between Longitudes 33^0 35/ 24// E and 330 45/E and Latitudes 26^0 43/ 43N// and 26^0 48/ 36//N (Figure 1). The area under investigation is studied by different authors e.g. Barron (1902), Sabet et al (1972), Akaad et al., (1973), Refeat et al (1977), Abu El Ela (1979), Kaoud (1982), Mahdy et al., (1994), Zalata et al (1996), and Abd El Aal (2009). The studied granite is one of the most promising uranium occurrences in the North Eastern Desert of Egypt because of its contents of abnormal high level of radioactivity.

The study area covers about 170 km^2, (Figure 1). It is characterized by rugged topography with moderate to high relief and very arid climate. The present work is concerned with geology of rock unites covering Wadi Ras Baroud area, as well as heavy mineral concentrations and radioactivity in the stream sediments covering the main wadies dissected the area.

The basement rocks of Ras Baroud area are of Precambrian age and dissected by dry wadi that filled by a wide variety of stream sediments (wadi deposits). These wadies deposits are composed of sands, gravels, and boulders. They are mainly derived from granites containing some variable heavy minerals.

Geologic Setting

The studied area is located in the North Eastern Desert of Egypt. The accessibility of the area is easy where the area is far from the Safaga City about 35km, and 21 km in Wadi Ras Baroud. The rock exposures are represented by older granitoides ranging from quartz diorites-granodiorites, syenogranites, and dissected by different types of basic and acidic dykes.

Quartz diorites-granodiorites

They composed from quartz diorite with predominance of granodiorite. They are medium-to coarse-grained containing numerous amounts of mafics. In some places, they attain high topography forming mountainous bodies with well-developed semi-rounded boulders that quarried as building stones.

These rocks are the most predominant rock types exposed in the area and covering about 70 % of the total mapped area. They occupy the eastern and southern parts of the mapped area as well as the northeast corner of the studied area. (Figure 1). The contacts between these rocks and syenogranites are intrusive (Figure 2a). Moreover, these rocks are dissected with basic and acidic dikes and characterized by the common presence of pegmatite dikes, pockets and vein.

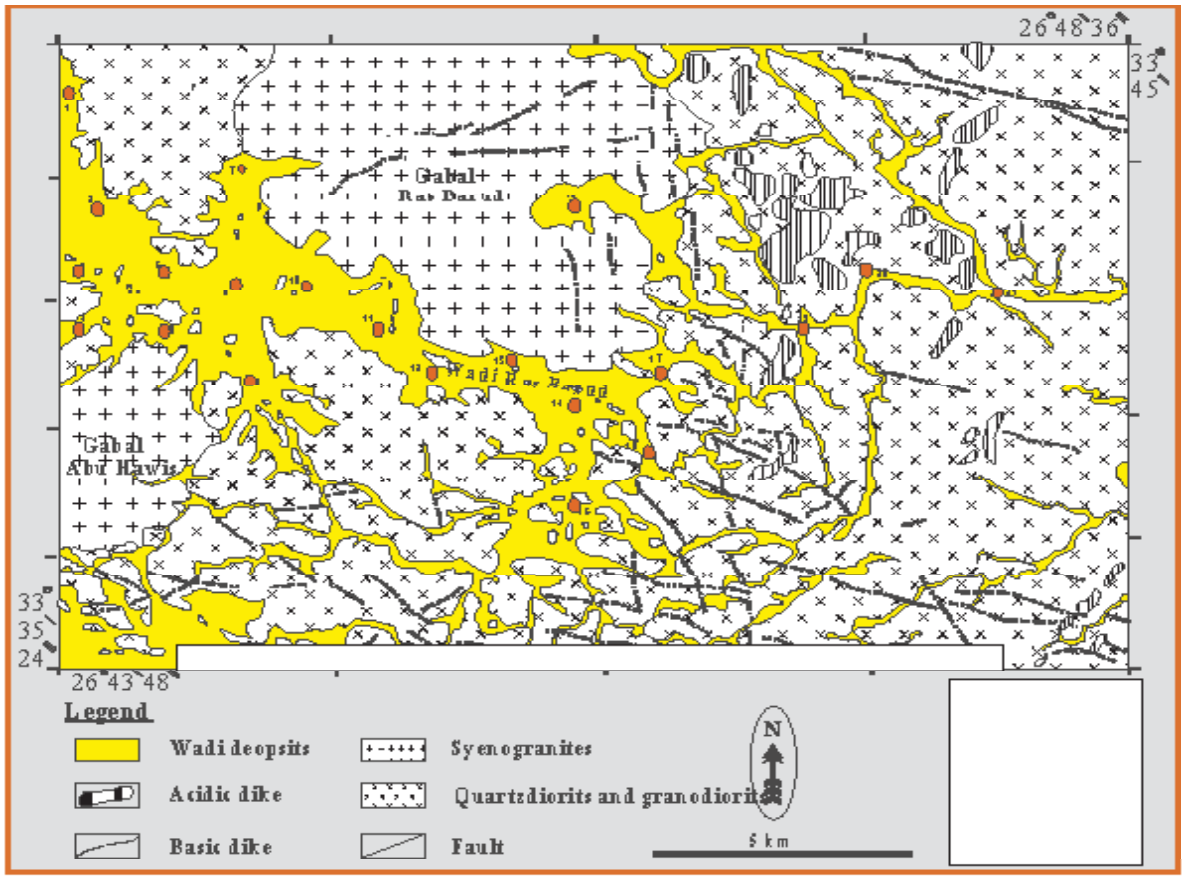

Figure 1 Geologic map showing the location of the collected samples in the study area

Syenogranites

The Ras Baroud syenogranites are medium to coarse-grained. These rocks are exposed as uniform masses of high relief in the northern part of the study area (Figure 1). They form, a stock-like body of semicircular outline having diameter of about 7km and an area of about 40km^2.

In general these granites are characterized by their red to pink color and massive nature, and exfoliation weathering (Figure 2b). The weathering surfaces are characterized also by a number of rounded to sub-rounded cavities of different diameters (Figure 2c).

These rocks intrude the quartz diorite-granodiorite with obvious intrusive contacts and roof-pendants (Figures 2a and 2d). These rocks are dissected by post granite dikes varying in composition from acidic, basic as well as pegmatites, and quartz veins (Figure 3a). Moreover, it is associated with several pegmatite pockets and veins especially along the southern and northern peripheries of G. Ras Barud (Figure 3b).

Dykes

The area under investigation is dissected by numerous dikes ranging in composition from acidic to basic. They emplaced along regional fractures of north-south, northeast-southeast, east-west and northwest-southeast directions (Figure 1). The cross-cut relationships of these dykes revealed that the acidic dykes are younger than the basic ones.

The acidic dikes are usually of great length extending more than 1km and their widths vary from 1m to 3m. These dikes are mainly quartz and micro-granodiorites, and less numbord of microgranite porphyries having northeast-southeast trend (Figure 3c).

The basic dikes are limited, reaching to 1 km in length and 1m in width. These dikes having N-S trends (Figure 3d). They are dark and composed of basalts.

Structure

Faults

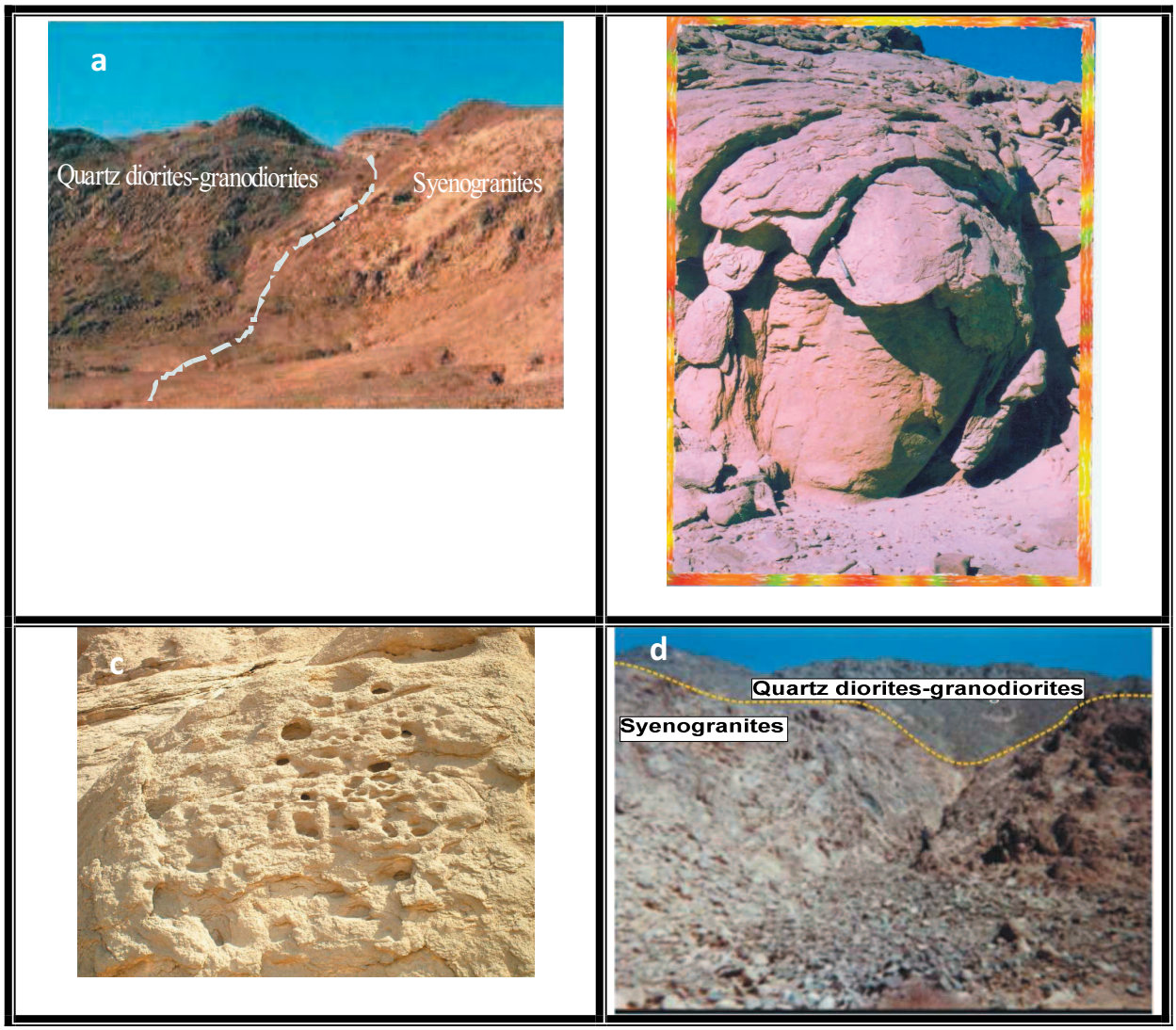

Figure 2: Photographs showing a) Sharp contacts between older and younger granites Wadi Ras Baroud, looking SE. b) X-foliation weathering in younger granites Gabel Ras Baroud, looking East. c) Rounded and subrounded cavities in younger granites Gabel Ras Baroud, looking SE. d) Younger granites intruding the older granitoids with obvious roofbendant, looking SE.

Faults are essential structural features in the study area (Figure 4). Slickensides and grooves are commonly associated with brittle faulting. These kinematic indicators clear the direction and sense of maximum resolved shear stress in that plane (Carey and Brunier, 1974). Slickensides are often composed of fibrous crystals of chlorite, epidote, calcite and quartz that stretch from one side of the fault plane to the other (Figure 5a). These faults are represented in both orders of sinistral and dextral senses of movement.

The strike-slip faults of N30°W trends are leftt-lateral (Figure 4). These strike-slip faults dislocate the intrusive rocks as Gabal Ras Baroud (Figure 5b). Fortunately, the rock exposures provided criteria to evaluate the activity along these faults in chronological order. The N30°W-trending faults are the oldest fracture planes, followed by the N70°W orientations. The NE-trending faults dislocate the older oriented faults.

These faults are determined by the features in the field study as slicken sides(Figure 5c), offset of rocks on two sides of fault plane, and affecting on the dikes and vine (Figure 5d).

Three main trends have been recognized which, in decreasing order of abundance, are N30°W, N70°W, and NE-SW as a minor trend. Measurements of the length and direction of these faults are grouped according to the total

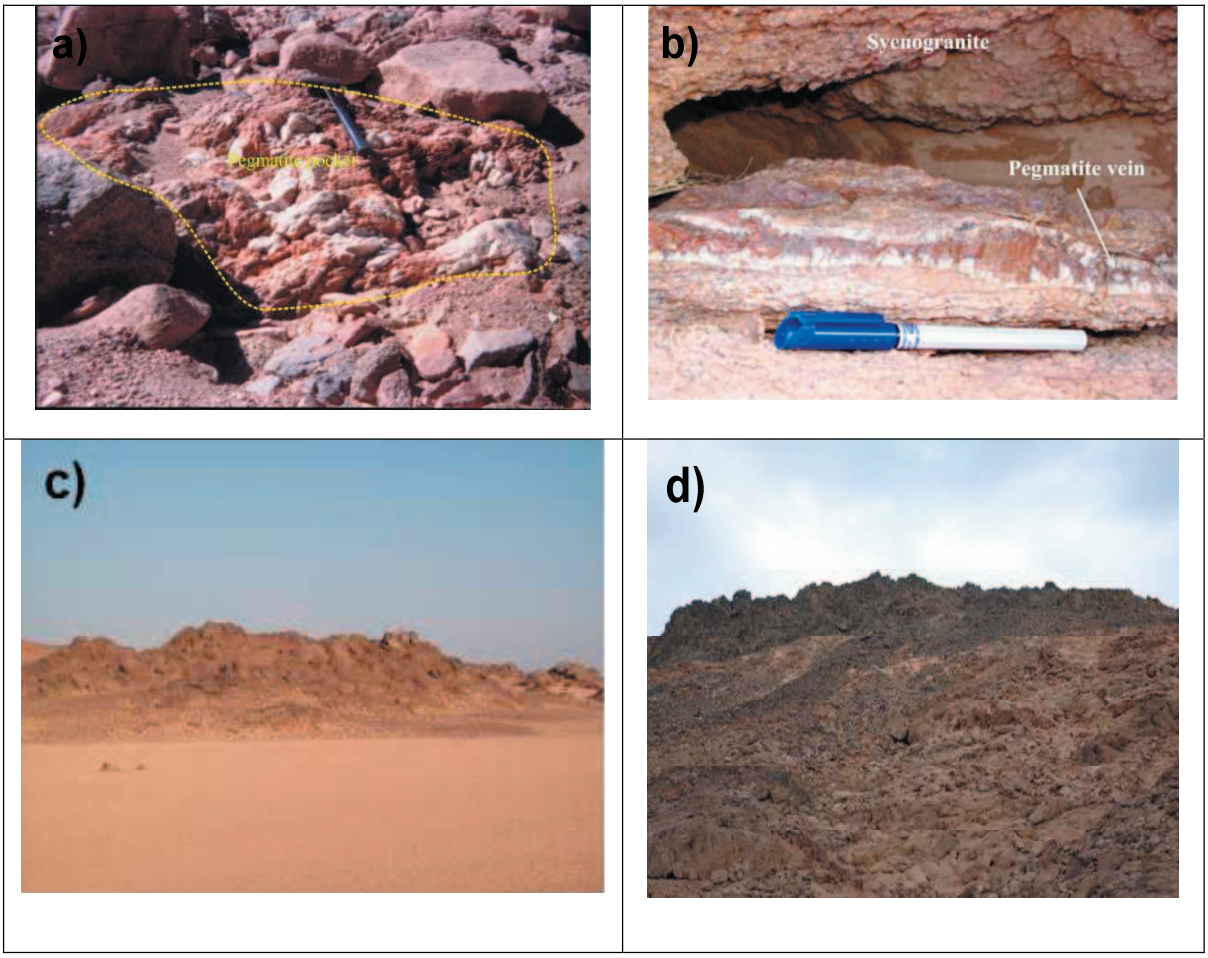

Figure 3: Photographs showing a) Small pegmatitic pocket in Gabal Ras Baroud, looking East. b) Pegmatite vein and cavities in syenogranite, looking East. c) Acidic dike trending NE-SW, looking NW d) Basic dikes trending N-S, looking E.

lengths and graphically presented by a rose diagrams

Three main trends have been recognized which, in decreasing order of abundance, are N30°W, N70°W, and NE-SW as a minor trend. Measurements of the length and direction of these faults are grouped according to the total lengths and graphically presented by a rose diagram (Figure 6). The wadi pattern in the area is one of the significant geomorphological features which show the effect of lithologic variations and structures. In the present work, all wadis and their tributaries were delineated and their lengths and directions were measured.

Materials and Methodology of Study

Twenty one channel samples were collected from the area around Wadi Ras Baroud from pore holes having about 50cm diameter, and 0.80-1m depth, with intervals ranging from 500-600m (Figure 1). The average weight of each sample is about 10kg. The air-dried original sample was sieved using 2 mm screen. The obtained fraction less than 2mm was quartered using June's splitters of different chutes, down to about 250 gm. Then the obtained representative sample is washed carefully several times to clarify it from silt and clay. Hydrogen peroxide was used to get rid of the organic matters.

A representative sub-sample weight about 60 gm was taken from each prepared sample by quartering and subjected to grain size analysis. The size analysis was carried out using a set of five standard screens selected according to the Wentworth Grade Scale having aperture diameters of 1.0, 0.5, 0.25, 0.125, 0.063 mm. The sieves were arranged in descending order with a receiver under the lower screen. The sets of screen with each sample on the upper one were shaked for about 30 minutes using a vibrating electric shaker.

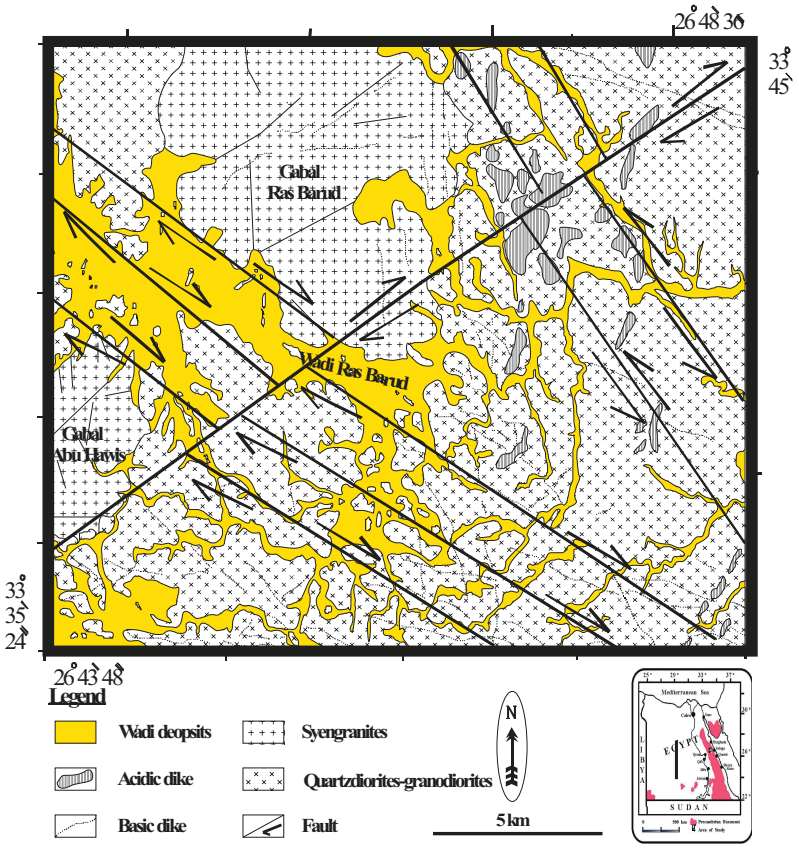

Figure 4 Structural map showing the major faults trends

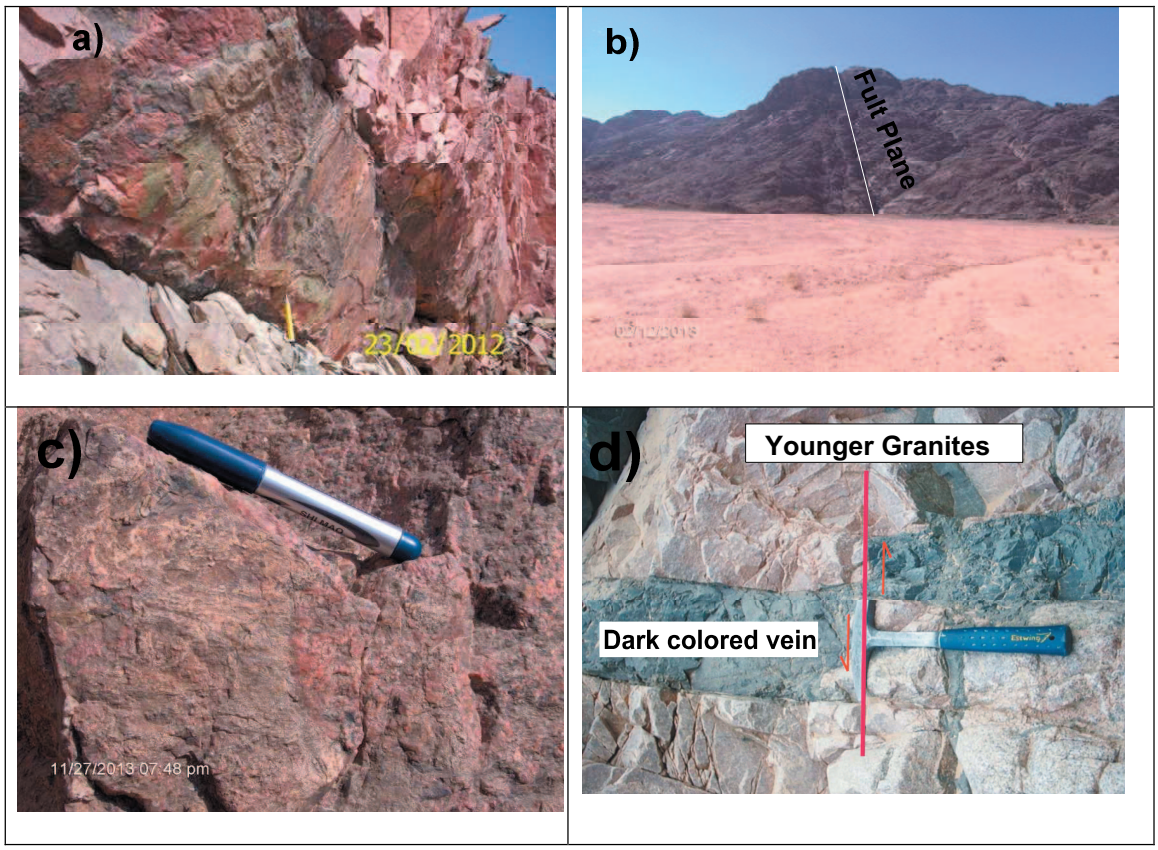

Figure 5 Photographs showing a) Slikenside with minor alteration features as epidotization restricted to fault planes, looking East. b) Faulting affecting Gabal Ras Baroud, looking SE. c) Horizontal slicken side for strike slip fault, looking East. d) dark colored vein affected by normal fault, looking East.

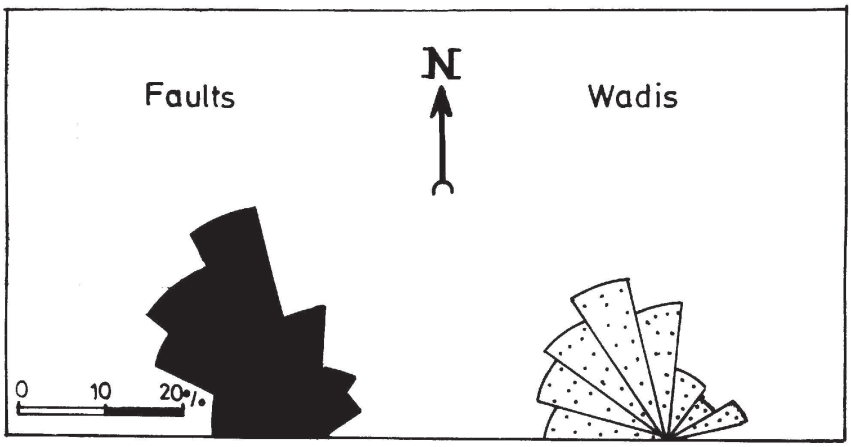

Figure (6): Rose diagram showing the main directional trends of wadis and faults

A representative sub-sample weighting about 60 gm was taken from each prepared sample by quartering for mineral separation. Separation was conducted using bromoform (Sp. Gr. 2.86o/gm cm^3) and magnetic fractionation using a Frantz Isodynamic Magnetic Separator (Model L-1). The obtained fractions were carefully studied using the Binocular Stereomicroscope.

In the present study, the collected 21 stream sediment samples were analyzed for some trace elements. The elements were determined by XRF techniques on pressed powder pellets. Mineralogical identification of the mineral constituents of the stream sediments was carried out by X-ray diffraction technique. A Phillips X-ray diffractometer (Model PW-1010) with a scintillation counter (Model PW-25623/00) and Ni filter was used. Semiquantitative EDX chemical analyses were carried out using a Phillips XL-30 Environmental Scanning Electron Microscope (ESEM).

The cylindrical plastic containers, of volume 212.6 cm^3, 9.5 cm average diameter, and 3 cm length. Then the container was filled with 300–400 gm of the samples, tightly sealed, and left for 30 days to accumulate free radon and attain radioactive equilibrium. The four standards eU, eTh, Ra, and K were measured twice, 1000 seconds for each; the average of gross counts was taken, then divided by their net weight, and introduced to a computer program (Matolin,1990), which runs under Ms-Dos to be used as a matrix of sensitivities represented as the concentrations of eU, eTh, Ra and K. These concentrations are used as a reference for the studied samples. The latter were measured in the same way by means of the computer program which gives out the concentrations of eU and eTh in ppm.

RESULTS AND DISCUSSION

Grain Size Analyses

The grain size analysis and their distribution is a fundamental descriptive measure for clastic sediments. It is an important parameter to understand and interpret the operative mechanism during transportation and reflect the sedimentary environments and the processes of sedimentation.

Inman (1952) suggested four formulae to measure the mean size, standard deviation (sorting), skewness and kurtosis taking into consideration the tailings of frequency curve of the grain size distribution.

The four different sedimentological statistical parameters were calculated for each sample, according to the equations quoted by Folk and Ward (1957) as follow:

- Graphic Mean (M_z) = (ϕ16 + ϕ50 + ϕ84) / 3

-Inclusive Graphic Standard Deviation (σ_I) = [(ϕ84 - ϕ16) / 4] +[ϕ95- ϕ5)/ 6.6]

-Inclusive Graphic Skewness (Sk_I) = [ϕ16 + ϕ84 – 2 ϕ50) / 2(ϕ84 - ϕ16)] + [(ϕ5 + ϕ95 - 2ϕ50) / 2(ϕ95 - ϕ5)]

- Graphic Kurtosis (K_G) = (ϕ95 - ϕ5) / 2.44 (ϕ75 - ϕ25)

The obtained results of the grain size distribution of the samples in the studied area showed the presence of clay, silt, sand and granule sizes. The sand size constitutes the main component of

all sample's deposit, the granule size was detected in few samples, while the clay and silt sizes contents is removed during decantation method.

The results of the calculated grain size parameters of the samples, and the description of these parameters according to limits of Folk and Ward (1957) were tabulated in (Table 1).

The samples have a graphic mean (Mz) ranging from 0.4φ to2φ (Table 1) which means that, it lies in coarse and medium sand size classes represented by 28.6% and 71.4% respectively (Table 1). The distribution of mean grain size of samples along the study area were represented in histogram (Figure 7a).

The samples have inclusive graphic standard deviation (σI) ranging from 1.2 to 1.9 (Table 1), the samples could be categorized in the poorly sorted class and represented by 100% (Table 1). The distribution of inclusive graphic standard deviation (σI) of samples along the study area were represented in histogram (Figure 7b).

The samples have inclusive graphic skewness (Sk_I) ranging from -0.3 to 0.22 (Table 1), the samples could be categorized in fine skewed, near symmetrical, and coarse skewed classes represented by 20% , 55%, and 25% respectively (Table 1). The distribution of inclusive graphic of skewness (Sk_I) samples along the study area were rep-

Table 1 The grain size parameters of the studied samples

Sample Name	Mean Size (Mz)		Standard Deviation (σ)		Skewness (SKI)		Kurtosis (KG)	
1	0.8	Coarse sand	1.4	Poorly sorted	-0.1	Near symmetrical	0.8	Platy kurtic
2	0.5	Coarse sand	1.7	Poorly sorted	-0.1	Near symmetrical	0.8	Platy kurtic
3	0.7	Coarse sand	1.5	Poorly sorted	0.0	Near symmetrical	0.7	Platy kurtic
4	0.8	coarse sand	1.6	Poorly sorted	0.0	Near symmetrical	0.8	Platy kurtic
5	0.9	Coarse sand	1.6	Poorly sorted	0.2	Near symmetrical	0.7	Platy kurtic
6	1.8	Medium sand	1.8	Poorly sorted	-0.2	Coarse skewed	0.7	Platy kurtic
7	1.5	Medium sand	1.5	Poorly sorted	0.0	Near symmetrical	0.8	Platy kurtic
8	1.3	Medium sand	1.6	Poorly sorted	0.0	Near symmetrical	0.8	Platy kurtic
9	1.2	Medium sand	1.4	Poorly sorted	0.2	Fine skewed	0.95	Meso kurtic
10	1.7	Medium sand	1.8	Poorly sorted	0.1	Near symmetrical	1.0	Meso kurtic
11	0.9	Coarse sand	1.7	Poorly sorted	0.17	Fine skewed	0.8	Platy kurtic
12	2.0	Medium sand	1.7	Poorly sorted	-0.3	Coarse skewed	0.98	Meso kurtic
13	1.8	Medium sand	1.8	Poorly sorted	-0.2	Coarse skewed	0.7	Platy kurtic
14	1.9	Medium sand	1.9	Poorly sorted	-0.22	Coarse skewed	1.0	Meso kurtic
15	1.5	Medium sand	1.9	Poorly sorted	-0.23	Coarse skewed	1.1	Meso kurtic
16	1.1	Medium sand	1.4	Poorly sorted	0.15	Fine skewed	0.92	Meso kurtic
17	1.6	Medium sand	1.5	Poorly sorted	0.2	Fine skewed	1.0	Meso kurtic
18	1.5	Medium sand	1.7	Poorly sorted	0.0	Near symmetrical	0.8	Platy kurtic
19	1.4	Medium sand	1.2	Poorly sorted	0.00	Near symmetrical	1.0	Meso kurtic
20	1.3	Medium sand	1.3	Poorly sorted	0.22	Fine skewed	1.1	Meso kurtic
21	1.7	Medium sand	1.5	Poorly sorted	0.16	Fine skewed	0.96	Meso kurtic
Ratio of Parameters								
	28.6%	Coarse sand	100%	Poorly sorted	28.6%	Fine skewed	52.4%	Platykurtic
	71.4%	Medium sand			47.6%	Near symmetrical	47.6%	Mesokurtic
					23.8%	Coarse skewed		

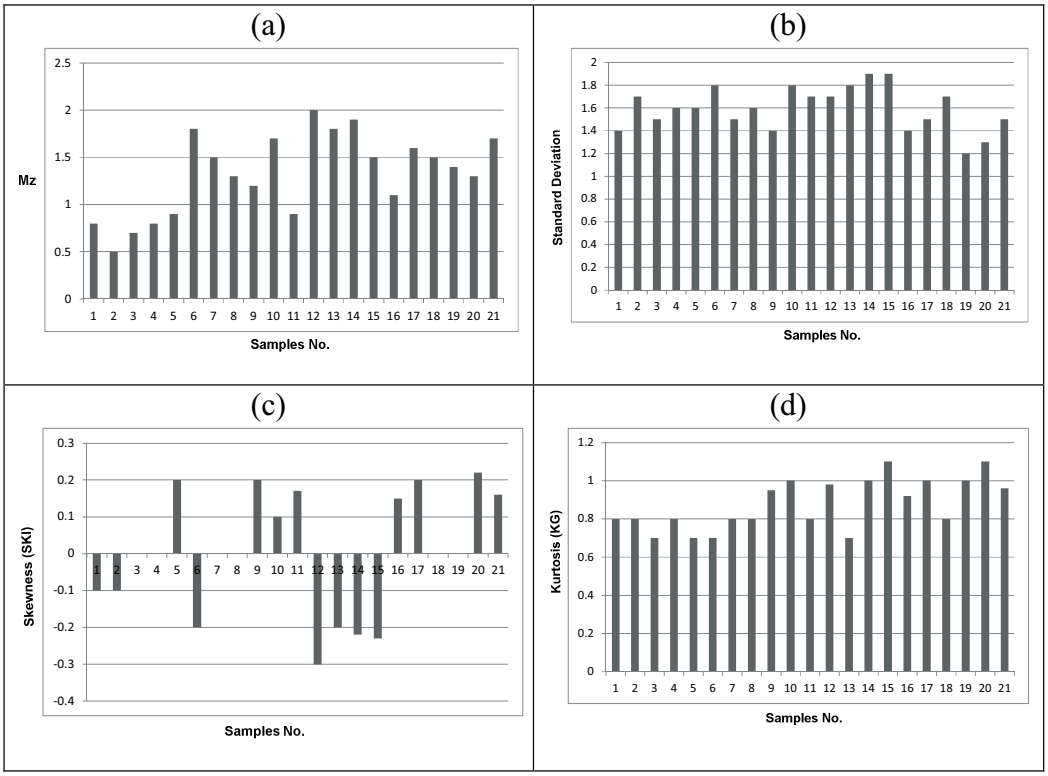

Figure 7 Histograms showing the distribution of a) Graphic mean M_z b) Inclusive graphic standard deviation (σ_I) c) Inclusive graphic skewness (Sk_I) d) Inclusive kurtosis (K_G)

resented in histogram (Figure 7c).

The samples have inclusive graphic kurtosis (K_g) ranging from 0.7 to 1.1 (Table 1), the samples could be categorized in the platykurtic and mesokurtic classes represented by 55% and 45% respectively (Table 1). The distribution of inclusive graphic kurtosis of samples along the study area were represented in histogram (Figure 7d).

From these parameters we can concluded that the sediments are characterized by medium to coarse grain size and poorly sorted, so it represents the turbidity currents environment.

Mineralogy

Magnetite (Fe_2O_4)

Magnetite was picked by hand magnet from the studied samples. It is characterized by an opaque and black color, rounded to subrounded grains and strongly magnetic (Figure 8a).

Ilmenite *([$FeTiO_3$])*

It is commonly angular to subrounded grains with metallic luster, black to brownish black colors (Figure 8b). Ilmenite is the most abundant Fe-Ti oxide mineral that occurs in a wide variety of igneous rocks.

Hematite (Fe_2O_3)

It is fine to coarse compact grains with brownish-red color, occurs as rounded to subrounded grains, separated at 0.5 amp. and originated from alteration of magnetite and pyrite (Figure 8c).

Rutile (TiO_2)

Rutile grains are subhedral to anhedral prismatic, tabular and elongated grains, varies in color from foxy red to reddish brown to opaque (Figure 8d). Rutile was recorded mostly in the non-magnetic fraction at 1.5 amp. and the magnetic fraction at 1.5 amp. Rutile is the preferred mineral for the production of titanium dioxide.

Garnet [$Fe_3Al_2(SiO_4)$]

Garnet which crystallizes in the isometric system, is mainly formed of angular to subrounded particles. Its grain size is relatively coarser than the other economic minerals of the study samples.

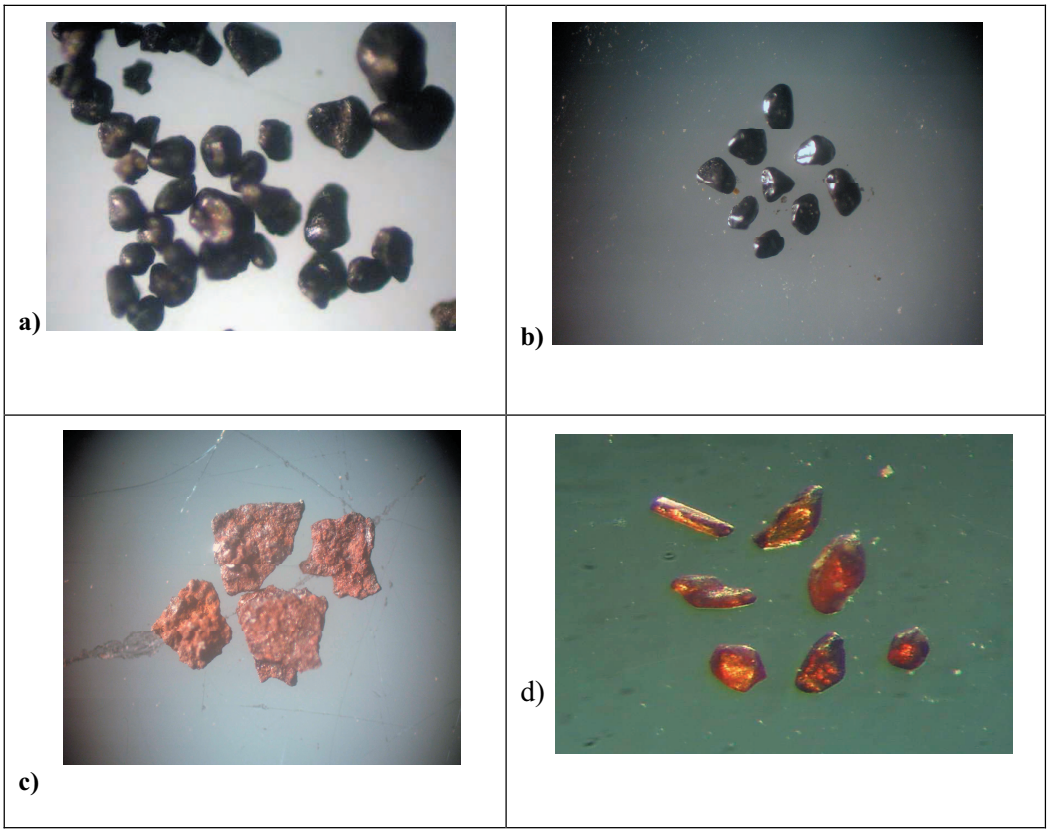

Figure 8: Photomicrographs of the recorded a) Magnetite b) Ilmenite c) Hematite d) Rutile

Garnet is the pale pink color (Figure 9a), and has moderate magnetic susceptibility which varies slightly according to variation in chemical composition (Milner, 1962).

Sphene (Titanite) [$CaTiSiO_5$]

Sphene is widespread in acidic and intermediate igneous rocks, and in several metamorphic rocks as accessory mineral. Titanite mineral grains are subhedral to anhedral of adamantine luster and imperfect cleavage. It exhibits transparent to translucent yellow to yellowish brown colors (Figure 9b).

Zircon [$ZrSiO_4$]

It occurs as subhedral to anhedral grains exhibiting colorless to brownish yellow colors of adamantine luster. Prismatic crystals are the prominent forms of zircon (Figure 9c), while few zircon grains are well preserved as euhedral crystals with bipyramidal termination. The EDX shows the chemical composition of zircon.

Thorite [$ThSiO_4$]

Thorite occurs in natural as a primary mineral chiefly in pegmatites. It also occurs as an accessory mineral in black sands and other detrital deposits derived from gneissic or granitic terranes. It occurs associated with zircon, sphene, monazite, xenotime, allanite, and various niobate-tantalates. It can vary in composition through the substitution of U, rare earths, Pb, Zr, Fe, and Ca chiefly, in variable and sometimes large amounts. Thorite almost has undergone extensive secondary alteration of both a structural and chemical nature. Structurally, the mineral may lose its crystallinity and assume a glasslike state in metamict state.

It occurs as brownish black to black opaque grains of greasy luster (Figure 9d). Most of thorite mineral grains are subhedral to anhedral corroded and cracked. Rarely, euhedral prismatic thorite grains are present. They are strongly metamictized, as determined by X-ray diffraction. Thorite was annealed at 1100˚C for approximately four hours preceding identification by XRD. The obtained data (Table 2) reveal the presence of thorite peaks (ASTM card 11-419) in addition to hematite peaks (ASTM card 13-534). The presence of hematite may be in the form of thin films coating thorite grains or as individual

Table 2: X-ray diffraction data of the annealed thorite from the studied stream sediments.

Analyzed Sample		Thorite ASTM card (11-419)		Hematite ASTM card (13-534)	
dA	I/Io	dA	I/Io	dA	**I/Io**
4.7	59	4.72	85		
3.56	100	3.55	100	3.66	25
2.83	21	2.842	45		
2.68	32			2.69	100
2.66	46	2.676	75		
2.53	21	2.516	30	2.51	50
2.35	3	2.361	5		
2.22	22	2.222	30	2.201	30
2.06	2			2.07	2
2	12	2.019	20		
1.89	15	1.885	30		
1.80	28	1.834	65	1.838	40
1.8	10	1.782	20		
1.69	12			1.69	60
1.67	8	1.667	10	1.634	4
1.475	5	1.484	20	1.484	35
1.44	4	1.444	15	1.453	35

Table 3: X-ray diffraction data of the fergusonite from the studied stream sediments.

Analysed sample		Fergusonite (9-443)	
dA	I/I0	dA	I/I0
3.12	100	3.12	100
2.97	67	2.96	90
2.73	50	2.74	40
2.65	19	2.64	20
2.53	10	2.53	10
2.17	6	2.16	6
2.0	3	2.01	6
1.89	42	1.90	50
1.86	28	1.85	30
1.75	8	1.75	10
1.64	15	1.65	10
1.61	18	1.62	16
1.57	18	1.57	10
1.51	8	1.50	6
1.47	7	1.48	4

hematite grains. The EDX shows the chemical composition of thorite.

Fergusonite ($YNbO_4$)

These crystals are rectangular prisms, striated, velvety-black with brown surface alteration to bloody red . They are characterized by resinous luster, compact, metamict, hard and common in heavy minerals sands.

The XRD of the studied powder, after heating to 1000 ^{o}C for 3 hours, indicates that, the pattern comprises fergusonite (Table 3), (Figure 9e)

Columbite ($(Fe,Mn)(Nb,Ta)2O_6$)

Prismatic, stubby or tabular crystals, often in heart-shaped twins, striated, black with metallic appearance and sometimes coated with an iridescent film. Columbite crystals are generally of granular form (Figure 9f). Massive aggregates, epitaxial overgrowth of columbite and ferugonite occur. Columbite is isomorphous with tantalite and considers as an ore of niobium as well as a source of tantalum. When niobium predomi-

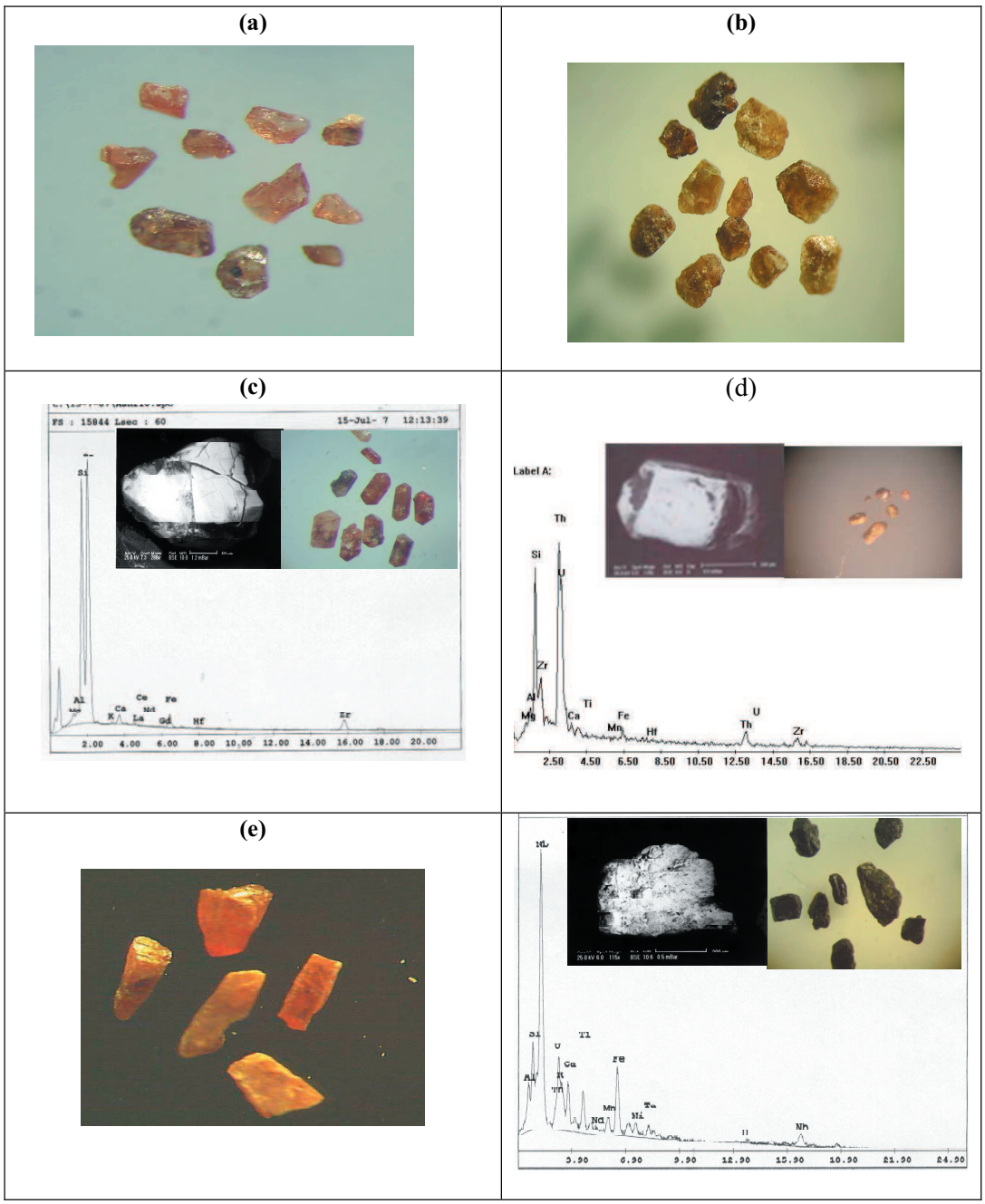

Figure 9: Photomicrographs of the recorded (a) Garnet (b) Sphene (c) Zircon (d) Thorite (e) Ferugsonite

nates, it is called columbite. The EDX shows the chemical composition of columbite.

Geochemical Study

Read (1984) mentioned that uranium is the most important trace element in zircon. The presence of high contents of U in zircon leads to the breakdown of the structure of zircon (metamict state), which causes radial and concentric fractures that are good pathways for uranium in addition to the presence of iron oxides (Moharem, 1999).

The results of XRF analysis of trace elements for these samples are tabulated in table (4). The table shows that, the stream sediments samples are rich in Zr, Ba and Sr, This clear that, the stream sediments are highly affected by the surrounding rocks. The distribution and lateral distribution of Zr and Nb elements are shown Figures 10a, 10b, 11a, and 11b. From these maps we can concluded that the concentration of Zr increases in the centeral part of the area around the syeno-granites. This indicates that the Zr does transported for large distance from the source or

Table 4: XRF Analysis of stream sediments samples

S. No.	Cr	Co	Ni	Cu	Zn	Zr	Rb	Y	Ba	Pb	Sr	Ga	V	Nb
1	73	22	30	69	74	560	60	8	352	7	1195	19	105	10
2	65	18	35	72	76	295	75	6	363	13	1167	24	88	7
3	80	26	27	71	65	480	74	7	390	11	885	20	95	9
4	71	21	26	76	87	275	84	15	328	15	852	23	81	7
5	60	24	19	65	85	335	250	75	281	16	284	21	65	20
6	65	19	23	61	95	345	92	35	278	8	725	22	71	18
7	75	20	25	74	105	265	80	12	329	9	945	25	82	9
8	67	22	22	69	99	250	68	37	265	6	692	18	78	19
9	74	18	21	65	115	510	102	68	260	14	697	26	71	38
10	62	17	26	70	80	299	140	25	320	13	745	27	82	20
11	55	20	19	60	155	805	163	148	248	18	175	25	76	94
12	45	21	25	65	204	509	174	117	232	19	200	28	91	69
13	55	18	25	69	133	442	117	55	285	12	455	19	79	53
14	30	26	35	67	209	1000	116	135	293	17	310	26	126	86
15	58	25	27	61	219	540	184	141	241	19	210	35	89	91
16	50	23	31	78	97	315	88	19	350	7	772	17	94	90
17	64	19	28	74	88	260	95	17	332	9	680	12	91	74
18	59	21	34	71	92	380	115	22	307	15	868	17	89	85
19	60	24	30	74	87	485	105	16	330	8	447	19	77	73
20	75	25	35	61	85	525	105	14	301	12	375	15	96	82
21	80	27	32	58	87	621	112	12	289	10	410	18	105	90

fare way from the source. The Nb distribution map shows increasing the Nb from up-stream to down-stream and indicates that, the Nb is transported fare from the source i.e. transported large distance from West to East.

Radiometric Study

A total of 21 stream sediment samples had been collected from the studied area throughout systematic sampling to determine their eU, Th, Ra and K contents. The obtained results from the radiometric measurements of the studied stream sediments are listed in Table 5.

The eU examined in the stream sediments of Wadi Ras Baroud ranges from 3 to 25 ppm (Figure 12a), while eTh ranging from 8 to 60 ppm (Figure 12b), Ra ranging from 3 to 19 ppm and K ranging from 0.9% to 3.3 %.

Ivanovich (1994) concluded that, a relatively constant eTh/eU mass ratio of around 3.5 is found in most natural systems, while the corresponding value obtained for this ratio ranging from 1.3 to 6.7. It indicates that there is a significant fractionation during weathering of these sediments causing the increasing or depletion of uranium in some samples.

The main factors controlling the distribution of radioelements in sediments are the geomorphological features of the basin of deposition, radioelements content of the source rocks, grain size of these sediments, the alkalinity of the surface groundwater, and to a lesser extent the effect of the organic matter. $^{238}U/^{226}Ra$ activity ratios (ARs) can be used to ascertain equilibrium within the same decay series (Navas et al., 2002). If secular equilibrium prevails in the ^{238}U chain, ARs of $^{238}U/^{226}Ra$ will be approximately 1,ARs values other than 1 indicate disequilibrium. The ARs for the studied stream sediments of Wadi Ras Baroud is higher than 1, which indicates a state of disequilibrium in these sediments.

eU versus eTh variation diagram

The relation between U and Th may indicate the enrichment or depletion of U because Th is normally stable. Thorium is three times as abundant as uranium in all rock types. When this ratio is disturbed, it indicates either depletion or enrichment of uranium.

Table 5 The distribution of radiomtric measurements of the studied stream sediments samples

Sample No.	eU (ppm)	eTh (ppm)	eTh/eU	Ra (ppm)	ARs eU/Ra)	K (%)
1	5	17	3.4	4	1.25	2.2
2	5	18	3.6	5	1	2.6
3	6	13	2.2	4	1.5	1.6
4	4	23	5.75	6	0.7	1.8
5	5	20	4	3	1.25	2.6
6	8	31	3.9	7	1.14	1.7
7	6	10	1.7	3	2	1.8
8	5	21	4.2	8	0.63	2.7
9	12	23	1.9	7	1.7	2.6
10	19	32	1.7	9	2.1	2.8
11	20	28	1.4	10	2	2.7
12	10	19	1.9	7	1.4	2.1
13	16	34	2.1	15	1.1	2.6
14	3	20	6.7	6	0.5	2.8
15	5	11	2.2	4	1.25	1.2
16	6	8	1.3	3	2	0.9
17	22	49	2.2	18	1.2	2.9
18	25	60	2.4	19	1.3	2.1
19	21	45	2.1	6	3.5	1.5
20	8	37	4.6	5	1.6	1.7
21	7	26	2.4	8	0.9	3.3

The eU against eTh variation diagram for the studied samples is shown in Figure (12c), which indicates strong positive relationships between these two elements. These results explain the low alteration processes affecting on these samples, and also indicates that magmatic processes played an important role in the uranium enrichment of these granites which represent the source of these sediments.

eU vs eTh/eU variation diagram

The bivariate diagram of eU against eTh/eU is shown in Figure (12d). This diagram, clear negative relationships for the studied samples. This relation may be either attributed to the mobilization of uranium in the studied samples.

eTh versus eTh/eU variation diagram

The relation between eTh and eTh/eU ratios is shown in figure (12e) for the studied samples. This Figure shows a scatter pattern which may be due to the effect of mobilization of (U) and concentration of (Th).

eU versus Zr variation diagram

The eU versus Zr variation diagram shows strong positive correlation in the studied samples (Figure 12f). The uranium and zirconium enrichment in the studied samples, supports the concept that U was trapped in the accessory minerals as zircon.

Conclusion

Ras Baroud area is covered by igneous rocks represented by quartz diorite-granodiorites and syenogranites and extruded by acidic and basic dikes. Grain size analyses revealed that, the grain size ranges from medium to coarse sand and poorly sorted. These samples are characterized by fine skewed, neer skewed , coarse skewed, platykurtic and mesokurtic. So, these sediments are represented by fluviatile and turbidity environments. The main representative minerals are iron oxides as magnetite, ilmenite, and hematite. Titanium minerals as rutile, abrasive minerals as garnet, radioactive minerals as zircon, sphene,

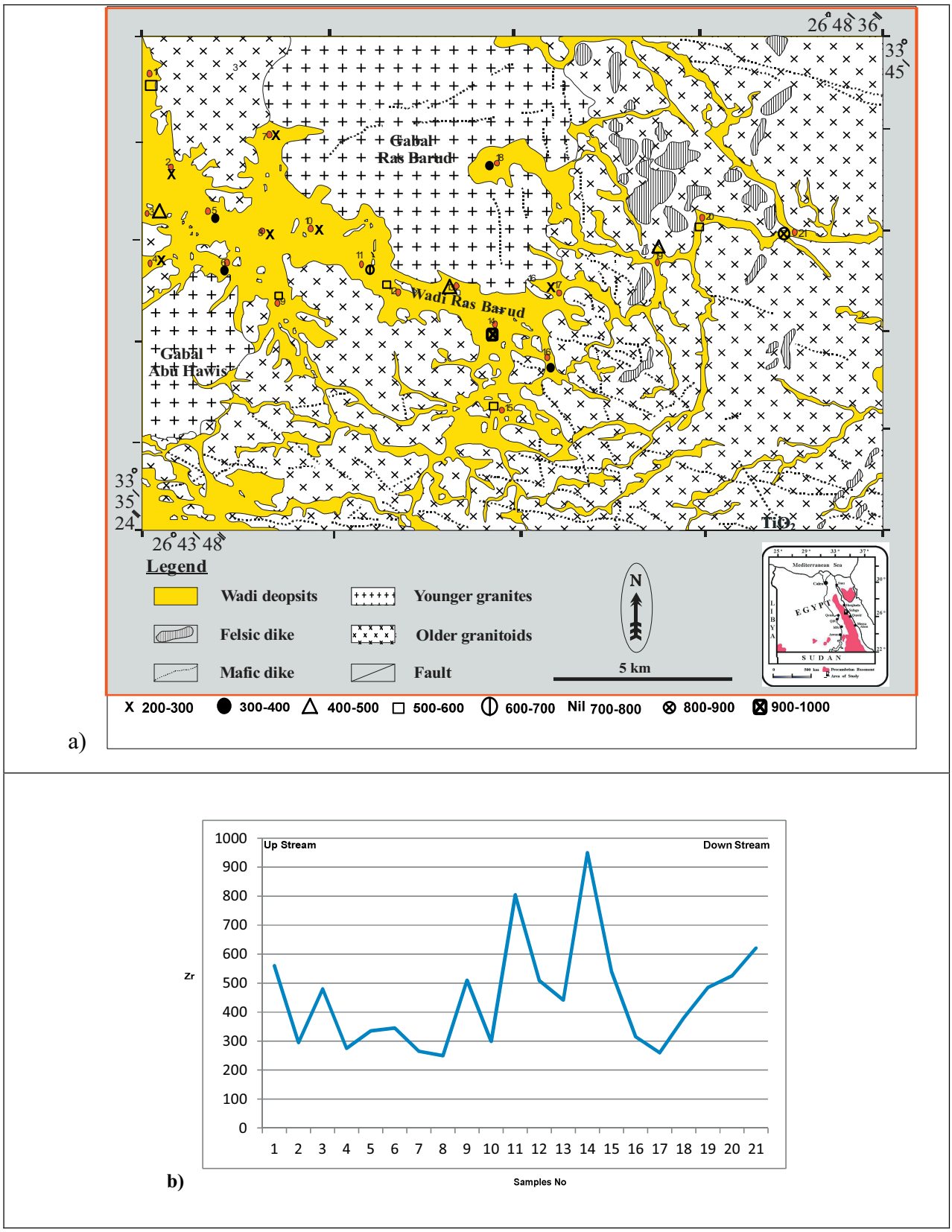

Figure 10 a)The distribution map of zircon in Wadi Ras Baroud area b) Lateral distribution of zircon

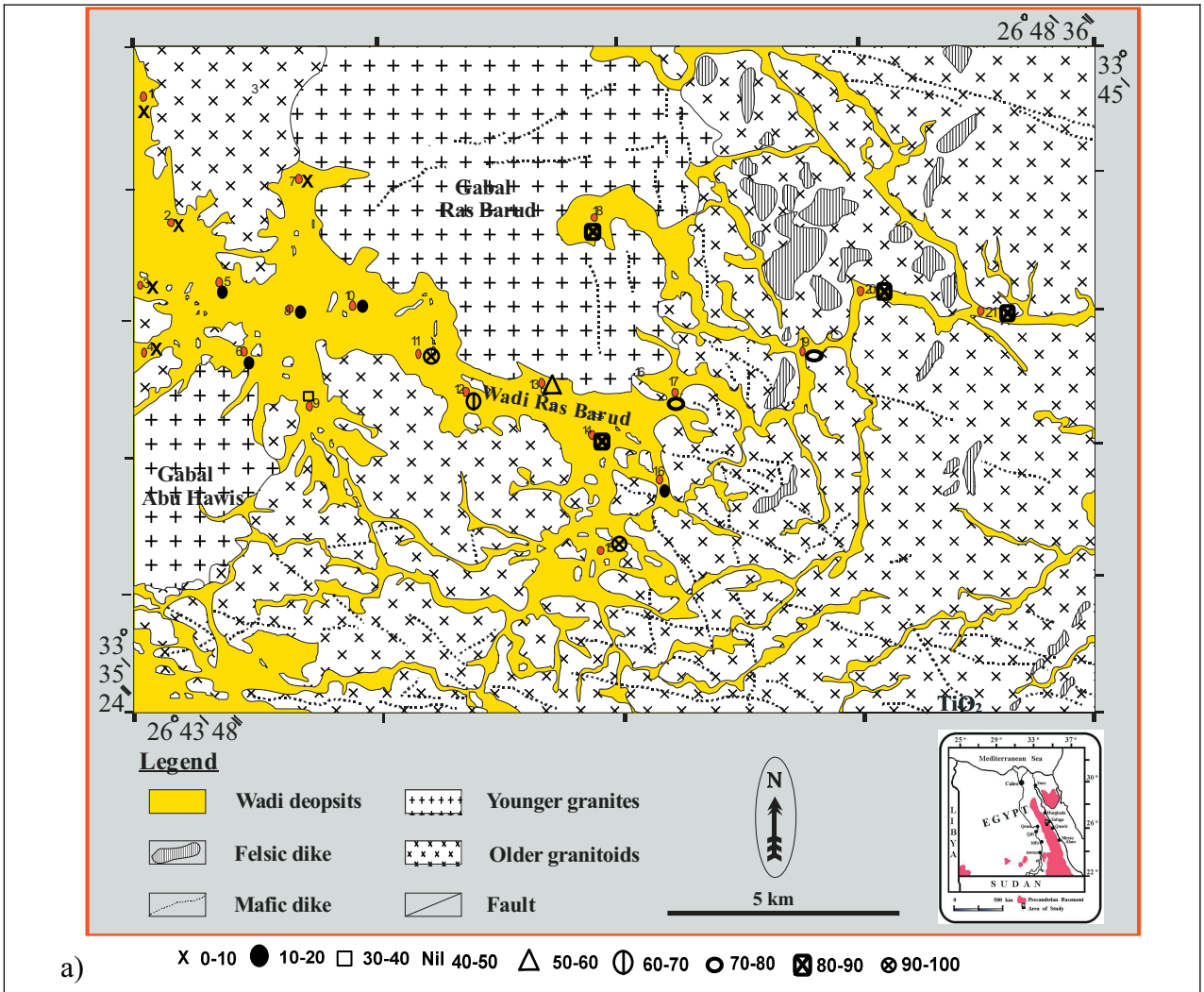

a)

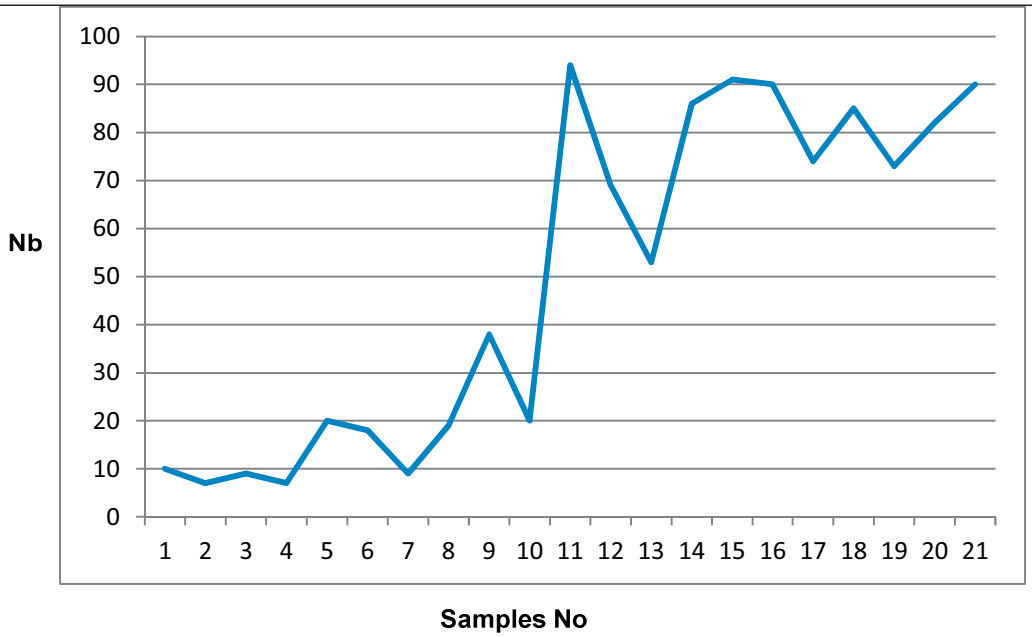

b)

Figure 11 a) The distribution of niobium **in Wadi Ras Baroud area b) Lateral distribution of** niobium

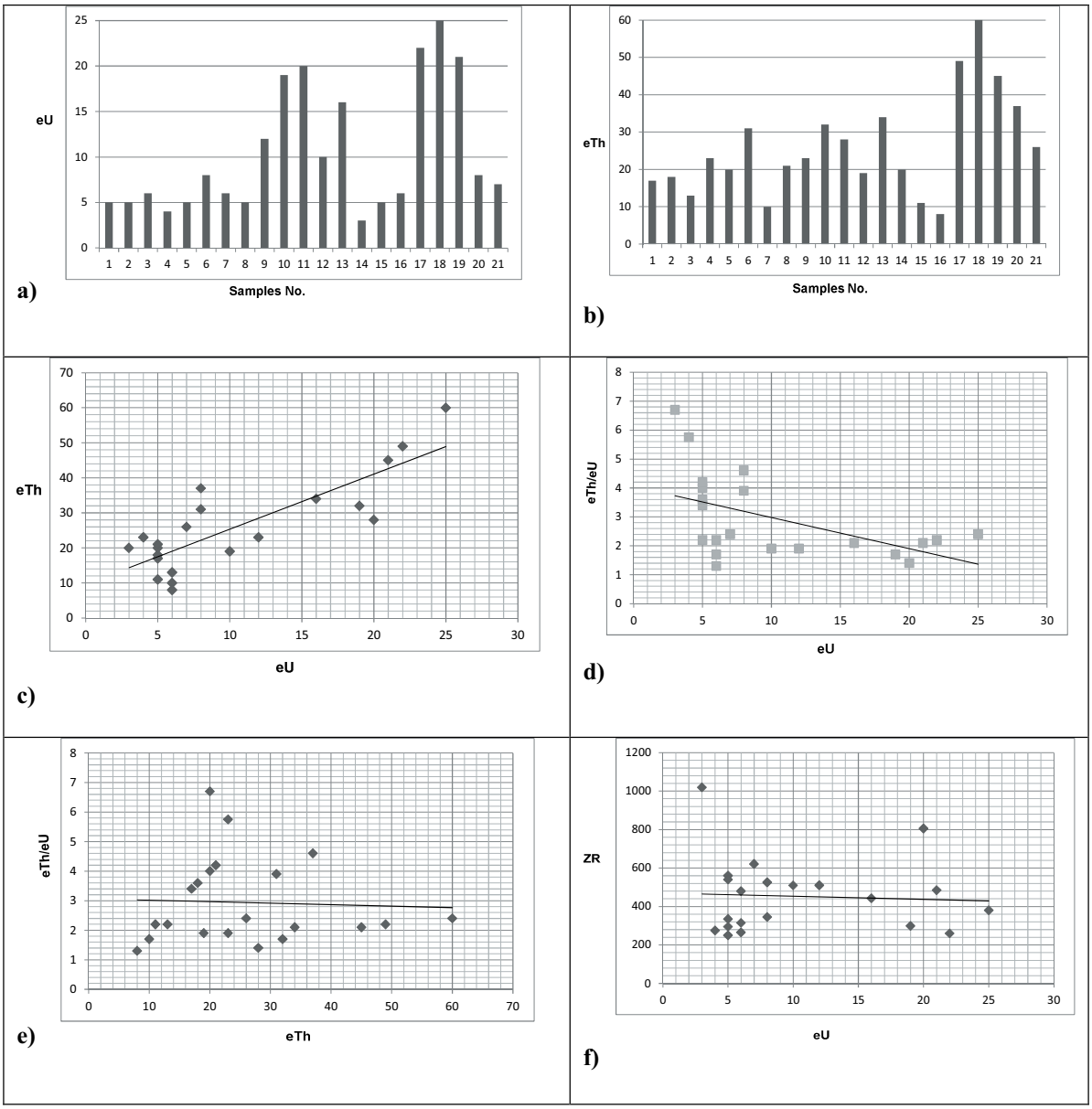

Figure 12: (a) and (b) Histograms showing the distribution of equivalent uranium and thorium ppm. (c) The relationship between equivalent uranium and equivalent thorium. (d) The relationship between eU and eTh/eU variation diagram for the stream sediments. (e) The relationship between eTh and eTh/eU variation diagram for the stream sediments. (f) The relationship between eU and concentration of Zr minerals.

thorite, ferogusonite, and columbite. The radiometric study of the stream sediments indicates that, the average concentrations of U and Th are 10.38ppm and 25.5ppm respectively. The ARs for the studied stream sediments are higher than 1, which indicate a state of disequilibrium in these sediments. The studied sediments are characterized by high concentration of (Th) and low concentration of (U).

REFRENCES

Abd El Aal, O.M., 2009. Radioactivity and geochemical prospection of stream sediments of Wadi El Baroud Area, North Eastern Desert, Egypt. Ph. D. Thesis, Faculty of Science, Tanta University, Egypt.

Abu El Ela, A. M. R., 1979. Geology of the Ras Baroud area, Eastern Desert. M. Sc. Thesis, Faculty of Science, Assiut University, Assiut, 193 p.

Akaad, M. K., El Gaby, S. and Habib, M. E., 1973. The Baroud gneisses and the origin of the grey granite. Bull. Fac. Sc., V.2, No.1, p. 55-68.

Barron, T. and Hume, W. F., 1902. Topography and geology of the Eastern Desert of Egypt (central portion) Geological Survey of Egypt, Cairo.

Carey, E., and Brunier, B., 1974. Analyse théorique et numérique d`un model mécanique

élémentaire appliqué à l'étude d`une population de failles. C. R. Acad. Sci. Paris, D 279, 891-894.

Folk, R. L., and Ward, W. C. 1957. Brazos River bar: a study in the significance of grain

size parameter. Jour. Sedim. Petrol., V. 27, pp. 3-27.

Inman, D. I. 1952. Measures for describing the size distribution of sediments: Jour. Sedim.

Petrol., V. 22, pp. 125-145.

Ivanovich, M. 1994. Uranium series disequilibrium: concept and applications. Radiochem.

Acta, Vol. 64, P. 81:94.

Kaoud, M. M. A., 1982. Conditions of formations of secondary dispersion geochemical anomalies of the rare metals in Ras Baroud, Eastern Desert, M. Sc. Thesis, Cairo University, A. R. E, 192 p.

Mahdy, M.A, Assaf, H.A, Abdel kader, Z.M, and Omaer, S.A 1994. Geological and

geochemical features of radioactive occurrences in gebel ras baroud granitic masses, central eastern desert, Egypt. Egyptian Mineralogist, Volum 6, P167-184.

Matolin, M., 1990. A report to the Government of the Arab Republic of Egypt

"Construction and use of spectrometric calibration pads", Egypt/4/030-03, Laboratory Gamma Ray spectrometry

Milner, H. B. 1962. Sedimentary petrography. V, II, George Allen & Unwin, Ltd., London. pp. 15-205.

Moharem, A. F. 1999. Geology and geochemistry and radioactivity of the area of Gabal El-Maghrabiya, central Eastern Desert, Egypt. Ph. D. Thesis, Faculty of Science, Ain Shams University, Cairo, Egypt, 211 p.

Navas, A., Soto, J. and Machin, J. 2002. 238U, 226Ra, 210Pb, 232Th and 40K activities in soil

profiles of the Flysch sector (Central Spanish Pyrenees). Applied Radiation and Isotopes. Vol. 57, P. 579:589.

Rafaat, A. M., Kabesh, M. T., and Abdallah, Z. M., 1977. Behavior of major elements in the granitic rocks of Ras Baroud, Safaga district, Eastern Desert, Egypt, J. Geol., 21, No.1, p. 35-61.

Read, H. H. 1984. Rutley's elements of mineralogy. Published by S. K. Jain for CBS Publishers and Distributors, Delhi, India, 560p.

Sabet, A. H., El Gaby, S., and Zalata, A. A., 1972. Geology of the basement rocks in the northern parts of El Shayib and Safaga sheets, Annal. Geol. Surv. Egypt, Vol. II.

Zalata, A., Mashaal, S. H., Ghobrial, G., El-Tokhi, M., and Makroom, F., 1996. Mineral chemistry and geochemical studies on Wadi-Al-Barud, Wadi Umm Taghir, Pan-African dyke swarms, Eastern Desert, Egypt. Egyptian Mineralogist. Vol. 8, p. 77-91.

اسهامات في معدنية واشعاعية رواسب الوديان بمنطقة
راس بارود, شمال الصحراء الشرقية- مصر

اشرف العزب - على احمد عمران - احمد حسان عبد المعبود

الملخص العربي

يقع وادى راس بارود في شمال الصحراء الشرقية. وتتمثل هذه المنطقة بصخور القاعدة الممثلة بالصخور المنكشفة في هذا الوادي تتكون من الجرانيتات القديمة وهى ممثلة بكوارتز ديوريت وجرانوديوريت اما الجرانيتات الحديثة تتمثل بسيانو جرانيت وجدد (مثل الحامضية والقاعدية) وتغطى هذه الاودية الرواسب الحديثة. ومن توزيع التدرج الحبيبي والعوامل الاحصائية لمعرفة خصائص هذه الرواسب نجد ان معامل التدرج ينحصر بين ٤و٠ Ø الى ٢و٠ Ø ومعامل الفرز ينحصر بين ٢و١ الى ٩و١ وهذا يدل على ان العينات متوسطة الى كبيرة الحبيبات وفقيرة الفرز. تم التعرف على بعض المعادن الثقيلة مثل الماجنتيت والمنيت والهيماتيت والجارنت والروتيل والتيتانيت والزيركون والثوريت والفيرجيوثونيت والكولمبيت. ومن دراسة رواسب الوديان اشعاعيا وجد ان متوسط تركيزات اليورانيوم والثوريوم ٣٨و١٠ جزء في المليون و٥و٢٥ جزء في المليون على التوالي.